

PET/CT imaging with a ¹⁸F-labeled galactodendritic unit in a galectin-1 overexpressing orthotopic bladder cancer model

Short title: ¹⁸F-Galactodendritic Carbohydrate for Bladder Cancer PET/CT

Patricia M. R. Pereira^{1,&}, Sheryl Roberts^{1,&}, Flávio Figueira^{2,3}, João P. C. Tomé⁴, Thomas Reiner^{1,5,6}, Jason S. Lewis^{1,5,7,8,9*}

& these authors contributed equally to this work.

Affiliations:

¹ Department of Radiology, Memorial Sloan Kettering Cancer Center, New York, NY 10065, USA

² QOPNA & LAQV-REQUIMTE, Department of Chemistry, University of Aveiro, 3810-193 Aveiro, Portugal

³ CICECO, Departamento de Química, Universidade de Aveiro, 3810-193 Aveiro, Portugal

⁴ CQE & Departamento de Engenharia Química, Instituto Superior Técnico, Universidade de Lisboa, Av. Rovisco Pais, n1, 1049-001 Lisboa, Portugal

⁵ Department of Radiology, Weill Cornell Medical College, New York, NY, USA

⁶ Chemical Biology Program, Memorial Sloan Kettering Cancer Center, New York City, NY, 10065, United States

⁷ Molecular Pharmacology Program, Memorial Sloan Kettering Cancer Center, New York, NY, USA

⁸ Department of Pharmacology, Weill Cornell Medical College, New York, NY, USA

⁹ Radiochemistry and Molecular Imaging Probes Core, Memorial Sloan Kettering Cancer Center,
New York, NY, USA

Corresponding author:

J. S. Lewis lewisj2@mskcc.org P: +1 646-888-3038, Fax: 646-888-3059

Immediate Open Access: Creative Commons Attribution 4.0 International License (CC BY) allows users to share and adapt with attribution, excluding materials credited to previous publications.



License: <https://creativecommons.org/licenses/by/4.0/>.

Details: <http://jnm.snmjournals.org/site/misc/permission.xhtml>.

ABSTRACT

Galectins are carbohydrate-binding proteins overexpressed in bladder cancer (BCa) cells. Dendritic galactose moieties have a high affinity for galectin-expressing tumor cells. We radiolabeled a dendritic galactose carbohydrate with fluorine-18 – ^{18}F -labeled galactodendritic unit **4** – and examined its potential in imaging urothelial malignancies.

Methods: The ^{18}F -labeled 1st generation galactodendritic unit **4** was obtained from its tosylate precursor. We conducted *in vivo* studies in galectin-expressing UMUC3 orthotopic BCa model to determine the ability of ^{18}F -labeled galactodendritic unit **4** to image BCa.

Results: Intravesical administration of ^{18}F -labeled galactodendritic unit **4** allowed specific accumulation of the carbohydrate radiotracer in galectin-1 overexpressing UMUC3 orthotopic tumors when imaged with PET. The ^{18}F -labeled galactodendritic unit **4** was not found to accumulate in non-tumor murine bladders.

Conclusion: The ^{18}F -labeled galactodendritic unit **4** and similar analogs may be clinically relevant and exploitable for PET imaging of galectin-1 overexpressing bladder tumors.

Keywords: dendritic carbohydrate, PET/CT imaging, bladder cancer, galectins, ^{18}F -radiochemistry

INTRODUCTION

Bladder cancer (BCa) is the tenth most prevalent cancer worldwide [1]. The GLOBOCAN 2018 estimated globally nearly 549,000 new BCa cases and about 200,000 deaths [1]. Most BCa arise in the bladder urothelium and are classified as urothelial carcinoma — also named transitional cell carcinoma (TCC) [2]. TCC represents more than 70% of patient cases and it is a non-invasive disease that commonly recurs in the urinary tract only. BCa muscle-invasive and metastatic disease, which is the lethal phenotype of BCa, occurs in nearly 20% of the patients [3].

BCa evaluation involves cystoscopy to collect a cell sample, a procedure named transurethral resection of bladder tumor (TURBT), followed by histological confirmation [4]. TURBT requires that the resection is deep enough to include the muscularis of the bladder to properly determine/stage whether the tumor is muscle-invasive or just *in situ*. Fluorescence cystoscopy and narrow-band imaging enhances cystoscopic detection of BCa due to their high specificity to the tumor tissue [5, 6]. CT, MRI urography, and ultrasound imaging have also demonstrated to enhance diagnostic accuracy in patients with BCa [7]. However, during tumor development, phenotypic alterations occur before morphological modifications are evident by cystoscopy, CT, MRI or ultrasound [8]. Positron Emission Tomography (PET) does not require tumor resection and may delineate these phenotypic alterations before morphological ones are apparent and therefore complement the use of TURBT. Tumor-targeting vectors bound to a positron emitting radionuclide (*e.g.*, fluorine-18) are widely used in oncology diagnostic imaging [8]. In this context, the glucose analogue 2-[¹⁸F]fluoro-2-deoxy-D-glucose (¹⁸F-FDG) accumulates in tumor cells as a result of their high glucose uptake mediated by glucose transporters (GLUTs).

Although ^{18}F -FDG PET/CT allows detection of metastatic disease, renal excretion of the glucose radiotracer results in difficulty identifying primary lesions of the bladder.

Recent studies have identified a role for galectins in BCa development and progression [9-12], suggesting their potential as biomarkers and providing clinical opportunities for the development of galectin-directed imaging and therapeutic approaches [13]. Galectins are a family of proteins containing carbohydrate-binding domains (CRD) with strong affinity for carbohydrate structures that consist of galactose residues [14]. Galectin-1 and galectin-3 are significantly upregulated in BCa compared to normal cells and contribute to tumor growth and invasion [13]. In a study with 185 BCa patient samples, 75% of the specimens demonstrated *LGALS1* (gene that codes for galectin-1) amplification and galectin-1 protein expression predicted disease-specific survival [11]. In addition, galectin-1 expression positively correlated with histological grade, pathological tumoral stage, and could discriminate between non-muscle invasive and muscle-invasive BCa [13]. Oligomerization of galectins results in CRD clustering and allows multivalent interactions with carbohydrates, resulting in the formation of ordered arrays (galectin-carbohydrate lattices) [15]. Tomé and coworkers previously developed a dendritic galactose unit to be conjugated with porphyrinoids [14] with high affinity for galectin-1 overexpressing BCa cells [16, 17]. Such a galactose dendritic molecule allows high affinity to tumor cells due to the ability of galectin-1 to establish multivalent interactions with the galactose units of the dendritic unit.

Here, we demonstrate the utility of the radiolabeled galactodendritic unit, ^{18}F -labeled galactodendritic unit **4**, to image galectin-1 overexpressing UMUC3 cells which were derived from human urinary bladder carcinoma and orthotopically implanted in the murine bladder.

METHODS

Chemicals were obtained from commercial suppliers and used without further purification unless otherwise stated. 2-mercaptoethanol, tetra-*n*-butylammonium fluoride, 4-toluenesulfonyl chloride, chemical reagents (DIPEA, triethylamine, potassium carbonate, sodium bicarbonate, and trifluoroacetic acid) and solvents (THF, DCM, acetone, chloroform-*d*, and HPLC and LC-MS grade acetonitrile) were purchased from Sigma-Aldrich (USA). Water (18.2 M Ω cm⁻¹ at 25 °C) was obtained from an Alpha-Q Ultrapure water system from Millipore (Bedford, MA). High-performance liquid chromatography (HPLC) purification and analysis were performed on a Shimadzu UFLC HPLC system with a DGU-20A degasser, an SPD-M20A UV detector, an LC-20AB pump unit, and a CBM-20A communication BUS module. All HPLC purification was carried out on a semi-preparative HPLC (Phenomenex Gemini C18, 5 μ m, 10 \times 250 mm, 3.5 mL/min 5–95% water/acetonitrile 10 min linear gradient) unless otherwise stated. Liquid chromatography-mass spectrometry (LC-MS) using electrospray ionization (ESI) was performed on Waters instrument with SQD detector for mass identification. A lyophilizer (FreeZone 2.5 Plus, Labconco, Kansas City, MO, USA) was used for freeze-drying. ¹H Nuclear magnetic resonance (NMR) and ¹³C NMR spectra were recorded on a Bruker AV 500 MHz at the Department of Chemistry in Aveiro, Portugal. ¹H NMR data are reported as follows: chemical shifts are in parts per million (ppm, δ) relative and are referenced to residual protic peaks. The coupling constants, *J*, are quoted in Hz and its multiplicities by s (singlet) d (doublet), t (triplet), q (quartet), m (multiplet) and br (broadened). ¹³C NMR are reported in parts per million relative to the solvent. All averages are presented as mean \pm standard deviation. Chromatograms and spectra were plotted on GraphPad software Prism 7 (San Diego, CA., USA).

Synthesis

Preparation of compound 1

2-[(4,6-bis(1,2:3,4-di-*O*-isopropylidene- α -D-galactopyran-6-yl)-1,3,5-triazin-2-yl)thio]ethan-1-ol.

In a 25 mL round-bottomed flask, di-galactotriazine (200.0 mg, 0.31 mmol, 1.0 equivalent) and DIPEA (0.17 mL, 0.95 mmol, 3.0 equivalent) were dissolved in 8 mL of dry THF and air purged with bubbling nitrogen for 15 min. The reaction was then cooled down in an ice bath. 2-mercaptoethanol (32.1 mg, 0.41 mmol, 1.3 equivalent) was added carefully to the reaction. The reaction was deemed finished after 3 h and purification on 20 \times 20 cm TLC plates with a 0.25 mm silica developed using ethyl acetate : hexane (1:1), furnished 173.0 mg (85%) of **1** as a colorless oil. ¹H NMR (500 MHz, chloroform-*d*) δ 5.55 (d, *J* = 5.0 Hz, 2H), 4.64 (dd, *J* = 7.9, 2.5 Hz, 2H), 4.53 (d, *J* = 6.5 Hz, 4H), 4.40 – 4.30 (m, 4H), 4.24 – 4.14 (m, 2H), 3.89 (t, *J* = 6.2 Hz, 2H), 3.32 (t, *J* = 6.2 Hz, 2H), 1.52 (s, 6H), 1.46 (s, 6H), 1.35 (s, 6H), 1.33 (s, 6H). ¹³C NMR (126 MHz, Chloroform-*d*) δ 184.8, 170.4, 109.6, 108.8, 96.3, 70.6, 70.6, 70.5, 66.5, 65.5, 61.9, 33.0, 26.1, 26.0, 24.9, 24.4. t_R = 13.35 min. ESI-MS: *m/z* calculated for C₂₉H₄₃N₃O₁₃S: 673.25; found: 674.3 [M + H]⁺.

Preparation of compound 2

2-[(4,6-bis(1,2:3,4-di-*O*-isopropylidene- α -D-galactopyran-6-yl)-1,3,5-triazin-2-yl)thio]ethan-1-oxytosylate.

Compound **1** (15 mg, 22 μ mol, 1.0 equivalent) and 4-toluenesulfonyl chloride (13 mg, 33 μ mol, 3 equivalent) were dissolved in 250 μ L of dichloromethane. The solution was cooled to 0 $^{\circ}$ C using an ice/acetone bath. Once cooled, a cold solution of triethylamine (12 μ L, ρ = 0.726 g/cm³,

88 μmol , 4 equivalent) in 250 μL dichloromethane was added dropwise. The reaction mixture was stirred at 0 $^{\circ}\text{C}$ until the ice/acetone bath melted and allowed to stir at room temperature overnight. The reaction mixture was dried *in vacuo*, resuspended in 250 μL acetonitrile with 5% water and HPLC purification afforded 15.66 mg (85%) of **2**. $t_{\text{R}} = 9.33$ min. ESI-MS: m/z calculated for $\text{C}_{36}\text{H}_{49}\text{N}_3\text{O}_{15}\text{S}_2$: 827.26; found: 828.63 $[\text{M} + \text{H}]^+$.

Preparation of compound 3

2-[(4,6-bis(1,2:3,4-di-O-isopropylidene- α -D-galactopyran-6-yl)-1,3,5-triazin-2-yl)thio]ethane-1- ^{19}F fluorine.

Compound **2** (1.17 mg, 1.41 μmol , 1.0 equivalent) and potassium carbonate were dissolved in 300 μL of acetonitrile before adding tetra-*n*-butylammonium fluoride (18.56 mg, 71 μmol , 50 equivalent) in THF to the mixture. The reaction mixture was stirred at 90 $^{\circ}\text{C}$ for 10 min and diluted with acetonitrile. HPLC purification afforded 0.67 mg (72%) of **3**. $t_{\text{R}} = 12.11$ min. ESI-MS: m/z calculated for $\text{C}_{29}\text{H}_{42}\text{FN}_3\text{O}_{12}\text{S}$: 656.25; found: 656.50 $[\text{M} + \text{H}]^+$.

Preparation of compound 4

2-[(4,6-bis(α/β -galactose-6-yl)-1,3,5-triazin-2-yl)thio]ethane-1- ^{19}F fluorine

Compound **3** was treated with a solution of trifluoroacetic acid (TFA) and dichloromethane (9:1), followed by the addition of one drop of water (≈ 200 μL). The reaction mixture was allowed to stir at 60 $^{\circ}\text{C}$ for 20 min. The reaction was neutralized with sodium bicarbonate and diluted with 500 μL water. The resulting mixture purified by HPLC affording qualitative yield ($>97\%$) of **4**. $t_{\text{R}} = 3.40$ min. ESI-MS: m/z calculated for $\text{C}_{17}\text{H}_{26}\text{FN}_3\text{O}_{12}\text{S}$: 496.12; found: 496.98 $[\text{M} + \text{H}]^+$.

Radiosynthesis

A standard procedure to separate the [^{18}F]fluoride in a form suitable for nucleophilic fluorination was carried out, as previously described in detail [18, 19]. Radiosynthesis of [^{18}F]compound **4** and its deprotection were completed in two steps *in situ*, using HPLC purification of the final product **4** to ensure chemical and radiochemical purity and molar activity of > 0.407 GBq/ μmol . [^{18}F]compound **4** was prepared in dry DMSO (500 μL) by adding compound **3** (200 μg) to the vial used to dry the [^{18}F]fluoride. The vial was sealed, heated to 90 $^{\circ}\text{C}$ for 6 min under stirring. The solution was either diluted with 1 mL of water and purified by HPLC - obtaining the radioactive compound **3** in qualitative yields greater than 85% (non-decay-corrected, n.d.c) - or the reaction was carried out *in situ* by treating the solution with TFA:DCM (9:1), followed by the addition of one pipette drop of water. The reaction was allowed to stir for 20 min at 60 $^{\circ}\text{C}$. The reaction was then neutralized with sodium bicarbonate, diluted with 700 μL water, and purified on HPLC. The collected peak (3.40- 3.80 min) was diluted 10:1 with water, trapped on a Waters C18 Sep-Pak Light cartridge, eluted with 500 μL of ethanol, and diluted to $< 5\%$ ethanol with sterile normal saline. [^{18}F]compound **4** was obtained in 45% overall n.d.c. radiochemical yield (based on measuring isolated final product on a dose calibrator at the end of formulation), 99% radiochemical purity after purification, and molar activity of > 0.407 GBq/ μmol . The synthesis was performed manually, starting with 60 mCi of [^{18}F]fluoride as delivered by the cyclotron; radiochemical yield is calculated from the activity eluted from the anion exchange cartridge. The fraction collected during the first HPLC run was ≈ 3 mL. Cold chemistry was performed under slightly different conditions (see synthesis section). The synthesis was completed within ~ 1.5 half-lives from EOB.

The ^{18}F -FDG was obtained from the Nuclear Pharmacy at Memorial Sloan Kettering Cancer Center on the morning of injection.

Bladder cancer cell lines and cell culture

Human BCa cells UMUC3, HT1197, and T24 were obtained from the American Type Culture Collection (ATCC). The UMUC14 and RT112 BCa cells were obtained from Sigma-Aldrich and European Collection of Authenticated Cell Cultures (ECACC). The cells were cultured according to the recommendations of ATCC, Sigma-Aldrich or ECACC and used within passage number of 6.

Galectin-1 interaction assays, galectin-1 knockdown and binding studies in bladder cancer cells

A solution of galectin-1 (Sigma) at a concentration of 2 μM was titrated with increasing concentrations of [^{19}F]compound **4** (0 – 3.2 μM). The fluorescence emission spectra of the tryptophan residues in the galectin-1 protein were acquired for the wavelength range between 300 to 450 nm upon excitation at 280 nm. The fluorescence-quenching curve was obtained by plotting the tryptophan residues quenching (in percentage) against [^{19}F]compound **4** concentration. The dissociation constants (K_D) of the galactose-conjugates to galectin-1 were calculated using the Boltzmann sigmoidal model [20].

Galectin-1 was depleted in UMUC3 BCa cells using a pool of three target-specific 20–25 nt siRNA (Santa Cruz Biotechnology) following previously reported methodology [16, 17].

BCa cells (0.25×10^6) resuspended in 100 μL of ice-cold PBS were incubated with 0.037 MBq of ^{18}F -galactodendritic unit **4** during 1 h at 4 $^\circ\text{C}$ with gentle agitation. Cells were then centrifuged at

1400 g for 4 min at 4 °C and supernatant containing unbound radioactivity collected into an eppendorf labeled #1. Cells were washed twice with 1 mL of PBS, centrifuged and supernatants collected into an eppendorf labeled #2. The pellet was resuspended in RIPA buffer. The pellet and supernatants were measured for radioactivity on a gamma counter calibrated for ¹⁸F. The % of binding was calculated using the following formula:

$$\text{Radioactivity}_{\text{Pellet}} / (\text{Radioactivity}_{\text{Pellet}} + \text{Radioactivity}_{\text{Eppendorf \#1}} + \text{Radioactivity}_{\text{Eppendorf \#2}}) \times 100.$$

Protein concentration was determined using the Pierce BCA Protein Assay Kit (Pierce) and the % of binding was then normalized to the amount of protein.

Orthotopic bladder cancer model

All experiments involving animals were performed according to the guidelines approved by the Research Animal Resource Center and Institutional Animal Care and Use Committee at Memorial Sloan Kettering Cancer Center, NY, USA. Pereira PMR (first author of this manuscript) has a Category C accreditation for animal research given from Federation of European Laboratory Animal Science (FELASA) and in this study, we adhere to the animal research: reporting of *in vivo* experiments (ARRIVE) guidelines and to the guidelines for the welfare and use of animals in cancer research.

Bladder orthotopic models were developed by inoculating UMUC3 cells into the bladder of 8 - 10 week-old *nu/nu* female mice. The mice were purchased from Charles River Laboratories.

Mice were anesthetized by inhalation of 1-2% isoflurane (Baxter Healthcare) in an oxygen gas mixture and kept on a heated platform during catheterization procedures. An angiocatheter (24 G, Terumo Medical Products) and the area of catheterization were lubricated before inserting the catheter into the urethra. After full insertion, the catheter was lifted gently and kept in parallel to

the bench. To avoid peri-urethral leakage and reflux to the upper urinary tract, the urine was removed from the bladder by abdominal massage and by applying suction to the external end of the catheter. The bladder was flushed with 80 μ L of sterile phosphate-buffered saline (PBS) and pre-treated with 80 μ L of poly-L-lysine (Sigma) for 15 min. A single-cell suspension of 5×10^5 UMUC3 cells in 50 μ L of media was inoculated into the bladder via the urethra with the angiocatheter. To improve tumor cell uptake, the catheter-syringe assembly was left in place for 40 min. This methodology allowed us to obtain a tumor take rate of 90%. During the entire procedure, mice were kept under anesthesia for 2 h before the catheter-syringe assembly was gently removed from the urethra. The mice were monitored everyday for any signs of pain and distress, and ultrasound imaging was used to monitor tumor development.

Ultrasound imaging of the bladder tumor

At 7 and 15 days after the inoculation of UMUC3 bladder cancer cells, the developed bladder tumors were non-invasively imaged using the Vevo 2100 Imaging System (Visualsonics). The transducer was placed in the mid pelvic region of the animal in transverse orientation until the bladder (a large black structure) appeared in the pelvic region. The images were then acquired in B-mode: 40 MHz frequency, 100% power, 52 frame rate, 30.0 dB gain, 10 mm depth, 14.08 mm width, high line density, high sensitivity, 65 dB dynamic range, G5 display map, 50 brightness, and 50 contrast.

PET/CT imaging and acute biodistribution studies

At 15 days after the inoculation of UMUC3 bladder cancer cells, mice ($n = 3$ mice per group) were 1) intravenously administrated ^{18}F -labeled galactodendritic unit **4** (2.9 – 3.3 MBq) or 2)

intravesical administrated (i.e. instillation directly into the bladder via insertion of an urethral catheter) 14.7-15.3 MBq of ^{18}F -galactodendritic unit **4** or ^{18}F -FDG.

At 0.5, 1 and 2 h post-intravenous administration of ^{18}F -labeled galactodendritic unit **4**, PET images were recorded on an Inveon PET/CT scanner (Siemens).

At 30 min post-intravesical administration, mice were anesthetized with 1.5-2% isoflurane and the bladder was fully empty, flushed with PBS, and PET images were recorded (following previously reported methodology [21]) at 1 h after intravesical administration. All images were visualized in AMIDE 1.0.4 software (<http://amide.sourceforge.net>).

Acute biodistribution studies were performed at 2 h after intravenous injection of ^{18}F -galactodendritic unit **4** [21] and radioactivity associated with each organ was expressed as a percentage of injected dose per gram of organ (% ID/g).

^{18}F -galactodendritic unit **4 stability in a saline solution containing 10.5% (v/v) mice urine**

Stability studies were performed in a saline solution containing 10.5% (v/v) mice urine as this mimics the *in vivo* conditions used in the PET imaging studies after the intravesical administration of the radiotracer. In the time between emptying mouse bladder and performing PET imaging experiments, we observed 10 μL urine excretion (corresponds to 10.5% of bladder mouse capacity $\approx 105 \mu\text{L}$). Urine was collected from mice with UMUC3 orthotopic BCa. In a 170 μL of PBS was added 20 μCi (10 μL) of compound **4**. 20 μL of urine was added to the solution and shaken. Stability test was performed by reversed-phase HPLC with in-line radiation (Posi-RAM model 4, LabLogic) detection using a Kinetex Biphenyl column (Phenomenex, 150×4.6 mm; 5 μm particle size) and a mobile phase gradient of 5–20% acetonitrile (0.1% TFA) in water (0.1% TFA) over 20 minutes. Intact [^{18}F]compound **4** elutes at 12 minutes, 75% (derived from

radiotracer chromatogram) or 50% (derived from HPLC chromatogram) intact after 30 min incubation and a number of metabolites eluted at later time-points after 1 h (Full characterization provided in the SI). The percent (%) intact radiotracer and metabolites were obtained from calculating the area under the curve.

RESULTS

Radiosynthesis of ^{18}F -labeled galactodendritic unit **4**

In 2012, Tomé and coworkers prepared a 1st generation galactodendritic unit based on 2,4,6-trichloro-1,3,5-triazine (TCT) [14]. Herein, we have attempted these syntheses changing the terminal group in the spacer region to a hydroxyl group facilitating further manipulation (**Fig. 1**). The di-nucleophilic substitution of TCT by the galactose moiety was carried out as previously reported [14]. The reaction of the di-galactotriazine with 2-mercaptoethanol provided the first-generation dendritic unit **1** in ~85% yield (**Supplementary Fig. 1 to 4**). We chose to pursue the tosylation of compound **1** at its phenol position since affording compound **2** is the most facile route for subsequent nucleophilic substitution ($\text{S}_{\text{N}}2$) of fluorine. This is especially important since the incorporation of its radioactive analog [^{18}F]F allowed the shortest amount of time for handling radioactive material. The small conversion of this group to an alkyl ether was predicted not to perturb targeting and galectin binding as we are not altering the hydroxyl groups in the carbohydrate moiety responsible for galactose binding to galectins [14, 16, 17]. The tosylation of compound **1** with 4-toluenesulfonyl chloride produced the desired product **2** in 85% yield. Compound **2** was reacted with tetra-*n*-butylammonium fluoride to produce [^{19}F]compound **3**. The subsequent deprotection of compound **3** gave the desired product, which eluted at 3.40 min on the reverse phase HPLC column, indicating good separation from compound **3**. We confirmed the chemical identity of all products (**Supplementary Fig. 5 to 7**).

The production of ^{18}F -labeled compound **4** was completed following a well-established [^{18}F]fluoroethylation, similar to previously described work [18, 19] (**Fig. 1**). The synthesis was

completed with 45% radiochemical yield (n.d.c.), with 99% radiochemical purity after purification. ^{18}F -labeled compound **3** could be isolated in a qualitative radiochemical yield greater than 85% (n.d.c.) and co-eluted with [^{19}F]compound **3** at 12.11 min on HPLC (**Fig. 2**). [^{18}F]compound **4** co-eluted with [^{19}F]compound **4** at 3.40 min on HPLC, confirming their chemical identity (**Fig. 2**).

^{18}F -labeled galactodendritic unit **4 binds to bladder cancer cells containing high levels of galectin-1 protein**

Porphyrinoids attached to the galactodendritic unit **4** have demonstrated in previous studies the ability to target galactose-binding proteins, such as galectin-1, overexpressed in tumor tissues [16, 17]. The [^{19}F]compound **4** interacts with galectin-1 protein (**Supplementary Figs. 8,9**), showing values of K_a and n equal to $8.778 \times 10^7 \text{ M}^{-1}$ and 1.0, respectively, as well as a K_D equal to $0.067 \pm 0.01 \mu\text{M}$.

To determine the ability of ^{18}F -labeled galactodendritic unit **4** to accumulate in bladder cancer cells, galactose radiotracer cell uptake was determined in five different bladder cancer cells containing different levels of galectin -1 (**Fig. 3A**). Notably, ^{18}F -labeled galactodendritic unit **4** binding to bladder cancer cells depends on galectin-1 protein levels. In comparison to UMUC14 and RT112 cells containing low levels of galectin-1, ^{18}F -labeled galactodendritic unit **4** displayed higher cell accumulation in galectin-1 overexpressing UMUC3 cells (**Fig. 3B**). Additional binding studies demonstrated that siRNA-mediated knockdown of galectin-1 (**Supplementary Fig. 10**) decreased ^{18}F -labeled galactodendritic unit **4** binding to UMUC3 cells (**Fig. 3C**).

¹⁸F-labeled galactodendritic unit 4 allows imaging of orthotopic BCa

The ¹⁸F-labeled galactodendritic unit 4 has high binding to UMUC3 bladder TCC cells containing a high expression of galectin-1 (**Fig. 3**) [16, 17] and, therefore, UMUC3 cells were used to develop an orthotopic BCa model. UMUC3 cells, when seeded onto the mouse urothelium, resemble the clinical condition of NMIBC [22]. At 15 days after cells' inoculation, tumor development was evaluated by ultrasound imaging. UMUC3 cells could be detected growing into murine bladders (**Fig. 4**) and were used in subsequent experiments.

To determine the biodistribution profile of ¹⁸F-labeled galactodendritic unit 4, mice implanted orthotopically with UMUC3 BCa cells were intravenously administered with ¹⁸F-labeled galactodendritic unit 4. Notably, there was a significant radiotracer accumulation in excretory and metabolic organs (**Supplementary Fig. 11**), as well as in the bone, as a result of radiotracer catabolism and degradation (**Supplementary Fig. 12**).

To determine the ability of ¹⁸F-labeled galactodendritic unit 4 to image BCa, mice implanted orthotopically with UMUC3 bladder tumors were intravesical administered with ¹⁸F-labeled galactodendritic unit 4. At 30 min after administration, time at which stability studies demonstrated 75% intact (derived from radiotracer chromatogram) or 50% intact (derived from HPLC chromatogram) ¹⁸F-labeled galactodendritic unit 4 (**Supplementary Fig. 12**), the bladder was completely empty and flushed with PBS. Mice without tumors were used as a negative control, receiving an intravesical administration of ¹⁸F-labeled galactodendritic unit 4. PET imaging at 1 h post-administration, shows a significant difference in the uptake of ¹⁸F-labeled galactodendritic unit 4 between the tumor (**Fig. 4**) and non-tumor groups (**Supplementary Fig. 13**). In the tumor group, registration of the PET and CT images showed the localization of most remaining activity in the tumor region revealing targeting of galactodendritic unit 4 to UMUC3

BCa cells. Quantitation of PET images by analyzing regions of interest ($n = 3$ mice per group) demonstrate higher uptake SUV_{mean} in tumor mice (**Fig. 4**) *versus* the non-tumor control group (**Supplementary Fig. 13**), with values of 43.5 ± 4.2 *versus* 2.0 ± 0.4 , respectively. Additional studies demonstrated that the glucose radiotracer ^{18}F -FDG accumulates in UMUC3 orthotopic bladder tumors with SUV_{mean} of 10.5 ± 2.3 after intravesical administration of the glucose radiotracer (**Supplementary Fig. 14**). While ^{18}F -labeled galactodendritic unit **4** binds to galectin-1 overexpressing UMUC3 bladder tumors (**Fig. 4**), the glucose radiotracer ^{18}F -FDG is reabsorbed after intravesical administration and accumulates in the kidneys and heart (**Supplementary Fig. 15**).

DISCUSSION

^{18}F -FDG PET imaging in BCa is hampered by ^{18}F -FDG renal excretion and the interference of accumulated, renally excreted activity in the bladder interfering with tumor delineation. Additionally, bladder tumor imaging with ^{18}F -FDG PET is limited to the fact that not all malignant cells take up glucose. The radiotracers ^{11}C -choline, ^{11}C -methionine, and ^{11}C -acetate (all of which have minimal urinary excretion) have been investigated as alternatives to ^{18}F -FDG for PET/CT in BCa patients [23]. In the context of BCa PET imaging, our group has recently demonstrated in subcutaneous HT1197 bladder tumors the utility of an antibody-based approach using a carbohydrate-antigen (CA19.9)-specific human antibody HuMab-5B1 (MVT-5873) [24].

In previous work, we synthesized a galactose dendritic carbohydrate to be conjugated with porphyrinoids with high affinity to galectin-expressing BCa cells [14, 16, 17]. In preclinical models of BCa, we demonstrated improved tumor binding and efficacy of therapeutic compounds conjugated with such galactose moieties [16, 20]. In this study, we extended our prior work and radiolabeled dendritic moieties of galactose to generate a PET imaging agent for the diagnosis of galectin-1 overexpressing BCa. We demonstrated by PET imaging that ^{18}F -labeled galactodendritic unit **4** specifically accumulates in galectin-1 expressing UMUC3 tumors engrafted in the murine bladder (**Figs. 3,4**). Admittedly, despite the successful *in vivo* demonstration of an effective binding of ^{18}F -labeled galactodendritic unit **4** to UMUC3 bladder cancer cells, we were not able to determine the nonspecific binding of the galactose radiotracer, since we did not perform *in vivo* experiments using a bladder cancer cell line containing low levels of galectin-1. As we observed *in vitro* binding of ^{18}F -labeled galactodendritic unit **4** to

bladder cancer cells containing low levels of galectin-1 (**Fig. 3**), further studies are necessary to determine the galactose radiotracer ability to bind to other galactose-binding proteins overexpressed in BCa (such as galectin-3). Galectin-1 protein expression has demonstrated higher expression in muscle-invasive when compared with non-muscle invasive BCa [13] and, therefore, further studies will determine the ability of ^{18}F -labeled galactodendritic unit **4** to differentiate between non-muscle invasive and muscle-invasive disease.

Carbohydrate radiopharmaceuticals have favorable properties as PET imaging agents: low antigenicity, fast clearance, and tissue penetration [8]. However, their main problems are related to *in vivo* catabolism, accumulation in non-tumor tissues, and urinary excretion [8]. The F-18 radionuclide is an ideal short-lived PET isotope (half-life of 109.7 min) for labeling of carbohydrates. Additionally, the F-18 radionuclide is easily produced in biomedical cyclotrons. Thus, the F-18 containing galactodendritic unit **4** was synthesized from the corresponding tosylate precursor **2** in two synthetic steps which were carried out *in situ* and producing 45% RCY (n.d.c.). Similar to ^{18}F -FDG, intravenous administration of ^{18}F -galactodendritic resulted in renal excretion in the bladder and therefore, interfering with tumor delineation. To avoid radioactivity accumulation in the metabolic (mainly liver) and excretory organs (e.g. bladder) as a result of ^{18}F -galactodendritic unit **4** catabolism and excretion (**Supplementary Fig. 11**), we decided to perform an intravesical administration of the radiotracer. Intravesical administration of an imaging or therapeutic agent is attractive in bladder cancer because this route of administration is clinically approved for BCa using immunotherapeutic or chemotherapeutic agents and the direct delivery of the agent into the bladder can achieve high concentrations at tumor sites while reducing for systemic drug uptake. Intravesical administration PET/CT with

^{18}F -galactodendritic unit **4** demonstrated to be a powerful tool for orthotopic bladder cancer imaging (**Fig. 3**), showing low accumulation in a non-tumor model (**Supplementary Fig. 13**) and low reabsorption after intravesical administration (**Supplementary Fig. 15**). ^{18}F -FDG was also able to delineate the bladder tumors, suggesting a potential for the glucose radiotracer to image bladder tumors after intravesical administration.

The galactose carbohydrate is almost exclusively catabolized in hepatocytes and, therefore, the ^{18}F -labeled galactose has shown potential in the detection of hepatocellular carcinoma [25]. The ^{18}F -labeled galactodendritic unit **4** is also a potential imaging agent in hepatocellular carcinoma and further studies are planned in that direction. The ^{18}F -labeled galactodendritic unit **4** offers the ability of interaction with galectin-1 (**Fig. 3**), resulting in high ability to accumulate and image galectin-1 overexpressing bladder tumors (**Fig. 4**). ^{18}F -labeled galactodendritic unit **4** should prove as a hit-to-lead-to-candidate optimization for further synthetic improvements in its scaffold to enhance stability *in vivo*. From here, possible modifications around the ether bonds could develop more robust galactodendritic structures, resistant to metabolic degradation. In addition to bladder cancer imaging, further studies will explore the potential of intravesical administration of galactodendritic units for bladder cancer therapy using drug-, therapeutic isotope-, photoreactive-bound compounds.

CONCLUSION

A dendritic galactose moiety was radiolabeled with F-18 from the corresponding tosylate precursor, resulting in a carbohydrate radiotracer with high affinity to the tumor cells due to its binding with galectin. The ^{18}F -labeled dendritic galactose **4** demonstrated high potential as a diagnostic tool for imaging of galectin-1 overexpressing BCa.

Acknowledgements

The authors acknowledge the MSKCC Small Animal Imaging Core Facility, the Radiochemistry and Molecular Imaging Probe Core, which were supported by NIH, grant P30 CA08748. This study was supported in part by the Geoffrey Beene Cancer Research Center of MSKCC (JSL) and NIH NCI R35 CA232130 (JSL). We gratefully acknowledge Mr. William H. and Mrs. Alice Goodwin and the Commonwealth Foundation for Cancer Research and The Center for Experimental Therapeutics of Memorial Sloan Kettering Cancer Center. PMRP acknowledges the Tow Foundation Postdoctoral Fellowship. We wish to thank Fundação para a Ciência e a Tecnologia (FCT, Portugal), the European Union, QREN, FEDER through Programa Operacional Factores de Competitividade (COMPETE), QOPNA (FCT UID/QUI/00062/2019) and CQE (FCT UID/QUI/0100/2019) research units, financed by national funds through the FCT/MEC and when appropriate co-financed by FEDER under the PT2020 Partnership Agreement. The research contract of F. Figueira (REF. -168-89-ARH/2018) is funded by national funds (OE), through FCT. We thank Dr. Luke Carter and Valerie Longo for their help with image analyses and ultrasound image acquisition. Supplementary Fig. 8 was created with Biorender.

Disclosure

There are no conflicts of interest.

KEY POINTS

QUESTION: Can galectin-expressing bladder cancer be imaged with a new ^{18}F -labeled galactodendritic unit?

PERTINENT FINDINGS: A ^{18}F -labeled first-generation galactodendritic unit was obtained from its tosylate precursor. Intravesical administration of ^{18}F -labeled galactodendritic unit allowed specific accumulation of the carbohydrate radiotracer in orthotopic bladder tumors when imaged with PET. The ^{18}F -labeled galactodendritic unit was not found to accumulate in non-tumor murine bladders.

IMPLICATIONS FOR PATIENT CARE: The ^{18}F -labeled galactodendritic unit and similar analogs may be exploitable for PET imaging, as a complementary diagnostic technique, to detect galectin-1 overexpressing bladder tumors.

REFERENCES

1. Bray F, Ferlay J, Soerjomataram I, Siegel RL, Torre LA, Jemal A. Global cancer statistics 2018: GLOBOCAN estimates of incidence and mortality worldwide for 36 cancers in 185 countries. *Ca-Cancer J Clin.* 2018; 68: 394-424.
2. Mitra AP, Cote RJ. Molecular pathogenesis and diagnostics of bladder cancer. *Annu Rev Pathol-Mech.* 2009; 4: 251-85.
3. Parekh DJ, Bochner BH, Dalbagni G. Superficial and muscle-invasive bladder cancer: Principles of management for outcomes assessments. *J Clin Oncol.* 2006; 24: 5519-27.
4. Sanli O, Dobruch J, Knowles MA, et al. Bladder cancer. *Nat Rev Dis Primers.* 2017; 3.
5. Lotan Y. Promises and challenges of fluorescence cystoscopy. *Urol Oncol-Semin Ori.* 2015; 33: 261-4.
6. Naito S, Algaba F, Babjuk M, et al. The Clinical Research Office of the Endourological Society (CROES) multicentre randomised trial of narrow band imaging-assisted Transurethral Resection of Bladder Tumour (TURBT) versus conventional white light imaging-assisted TURBT in primary non-muscle-invasive bladder cancer patients: trial protocol and 1-year results. *Eur Urol.* 2016; 70: 506-15.
7. Babjuk M, Bohle A, Burger M, et al. EAU guidelines on non-muscle-invasive urothelial carcinoma of the bladder: update 2016. *Eur Urol.* 2017; 71: 447-61.
8. Gambhir SS. Molecular imaging of cancer with positron emission tomography. *Nat Rev Cancer.* 2002; 2: 683-93.
9. Canesin G, Gonzalez-Peramato P, Palou J, Urrutia M, Cordon-Cardo C, Sanchez-Carbayo M. Galectin-3 expression is associated with bladder cancer progression and clinical outcome. *Tumor Biol.* 2010; 31: 277-85.

10. Sakaki M, Oka N, Nakanishi R, Yamaguchi K, Fukumori T, Kanayama HO. Serum level of galectin-3 in human bladder cancer. *J Med Invest.* 2008; 55: 127-32.
11. Wu TF, Li CF, Chien LH, et al. Galectin-1 dysregulation independently predicts disease specific survival in bladder urothelial carcinoma. *J Urol.* 2015; 193: 1002-8.
12. Liu YD, Liu Z, Fu Q, et al. Galectin-9 as a prognostic and predictive biomarker in bladder urothelial carcinoma. *Urol Oncol-Semin Ori.* 2017; 35: 349-55.
13. Martinez-Bosch N, Rodriguez-Vida A, Juanpere N, et al. Galectins in prostate and bladder cancer: tumorigenic roles and clinical opportunities. *Nat Rev Urol.* 2019; 16: 433-45.
14. Silva S, Pereira PMR, Silva P, et al. Porphyrin and phthalocyanine glycodendritic conjugates: synthesis, photophysical and photochemical properties. *Chem Commun.* 2012; 48: 3608-10.
15. Rabinovich GA, Toscanol MA, Jackson SS, Vasta GR. Functions of cell surface galectin-glycoprotein lattices. *Curr Opin Struc Biol.* 2007; 17: 513-20.
16. Pereira PMR, Silva S, Ramalho JS, et al. The role of galectin-1 in in vitro and in vivo photodynamic therapy with a galactodendritic porphyrin. *Eur J Cancer.* 2016; 68: 60-9.
17. Pereira PMR, Silva S, Cavaleiro JAS, Ribeiro CAF, Tomé JPC, Fernandes R. Galactodendritic phthalocyanine targets carbohydrate-binding proteins enhancing photodynamic therapy. *Plos One.* 2014; 9.
18. Pirovano G, Roberts S, Brand C, et al. [18F]FE-OTS964: a small molecule targeting TOPK for in vivo PET imaging in a glioblastoma xenograft model. *Mol Imaging Biol.* 2019; 21: 705-12.

19. Kniess T, Laube M, Brust P, Steinbach J. 2-[¹⁸F]fluoroethyl tosylate - a versatile tool for building ¹⁸F-based radiotracers for positron emission tomography. *Medchemcomm.* 2015; 6: 1714-54.
20. Pereira PMR, Silva S, Bispo M, et al. Mitochondria-targeted photodynamic therapy with a galactodendritic chlorin to enhance cell death in resistant bladder cancer cells. *Bioconjugate Chem.* 2016; 27: 2762-9.
21. Pereira PMR, Sharma SK, Carter LM, et al. Caveolin-1 mediates cellular distribution of HER2 and affects trastuzumab binding and therapeutic efficacy. *Nature Commun.* 2018; 9.
22. van der Horst G, van Asten JJ, Figdor A, et al. Real-time cancer cell tracking by bioluminescence in a preclinical model of human bladder cancer growth and metastasis. *Eur Urol.* 2011; 60: 337-43.
23. Bouchelouche K, Turkbey B, Choyke PL. PET/CT and MRI in bladder cancer. *J Cancer Sci Ther.* 2012; S14.
24. Escorcia FE, Steckler JM, Abdel-Atti D, et al. Tumor-specific Zr-89 immuno-PET imaging in a human bladder cancer model. *Mol Imaging Biol.* 2018; 20: 808-15.
25. Horsager J, Bak-Fredslund K, Larsen LP, Villadsen GE, Bogsrud TV, Sorensen M. Optimal 2-[¹⁸F]fluoro-2-deoxy-D-galactose PET/CT protocol for detection of hepatocellular carcinoma. *EJNMMI Res.* 2016; 6: 56.

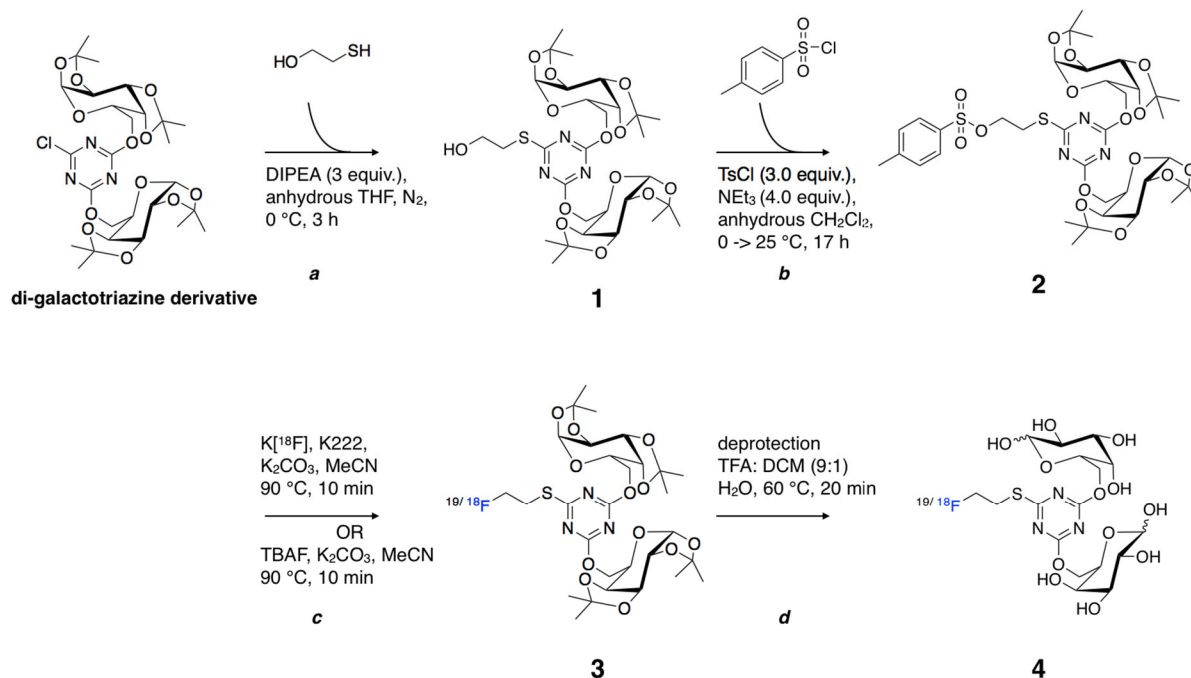


Figure 1. Synthetic reaction and conditions for the synthesis of [^{19}F]/[^{18}F] galactodendritic unit **4**. Reagents and conditions: (a) 2-mercaptoethanol, DIPEA, anhydrous THF, N_2 , 0°C , 3 h; (b) 4-toluenesulfonyl chloride, NEt_3 , anhydrous DCM, $0 \rightarrow 25^\circ\text{C}$, 17 h; (c) TBAF, K_2CO_3 , MeCN, 90°C , 10 min OR radiolabeling conditions activated $\text{K}^{[18\text{F}]}$, $\text{K}_{222}/\text{K}_2\text{CO}_3$, MeCN, 90°C , 10 min; (d) TFA:DCM (9:1), H_2O , 60°C , 20 min.

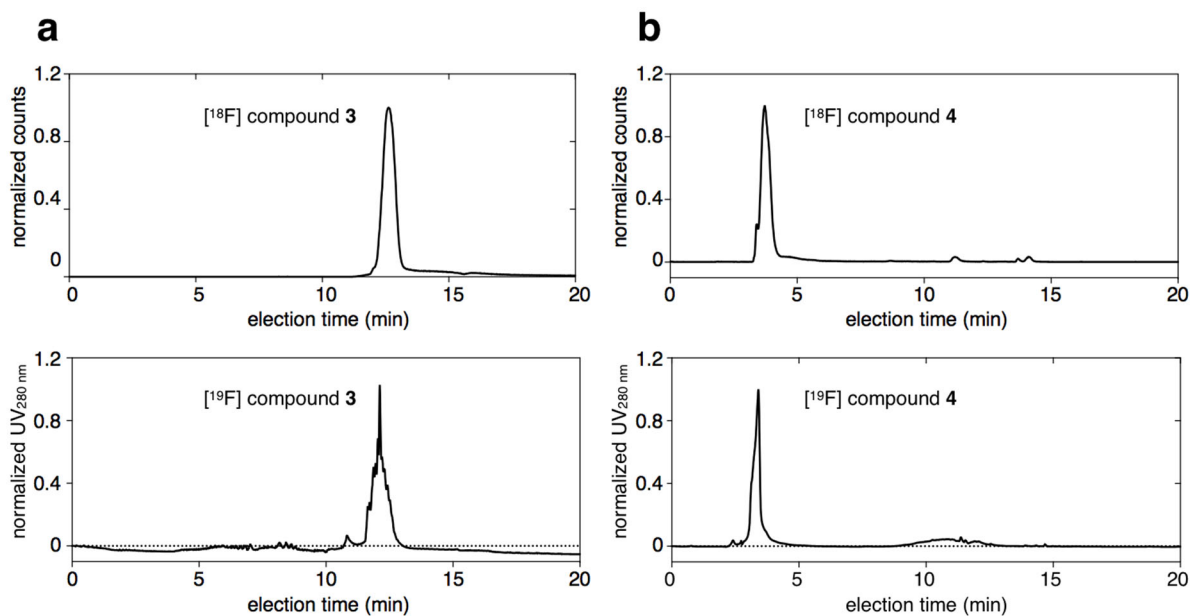


Figure 2. Confirmation for the chemical identity of $[^{18}\text{F}]$ galactodendritic carbohydrates **3** and **4** by HPLC using a verified cold standard. (a) Radio-HPLC chromatogram of $[^{18}\text{F}]$ galactodendritic carbohydrate **3** (*top*) and $[^{19}\text{F}]$ galactodendritic carbohydrate **3** (*bottom*). (b) Radio-HPLC chromatogram of $[^{18}\text{F}]$ galactodendritic unit **4** (*top*), co-eluted with $[^{19}\text{F}]$ galactodendritic unit **4** (*bottom*).

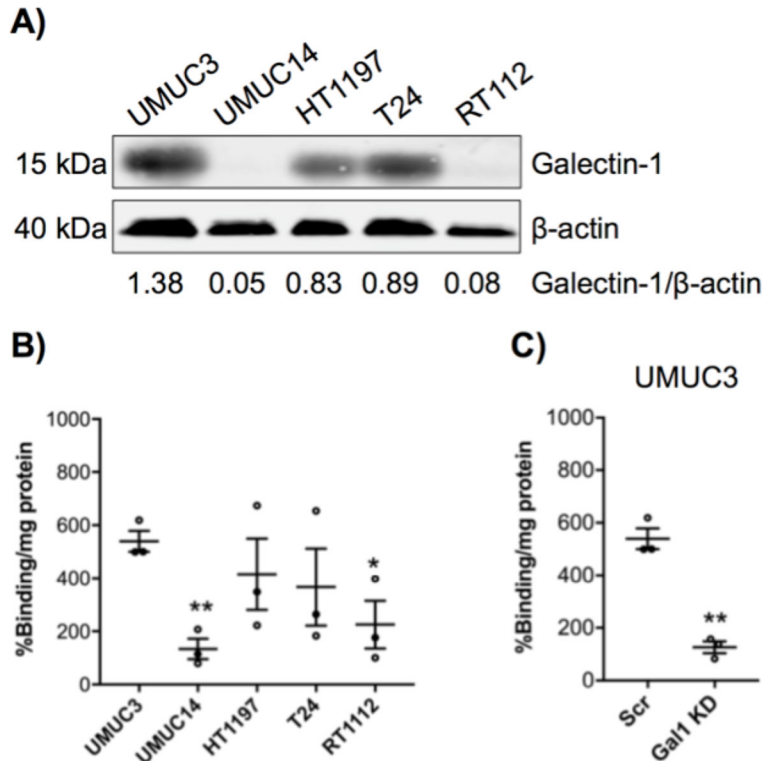


Figure 3. **A)** Western blot analysis of galectin-1 in the total lysates of UMUC3, UMUC14, HT1197, T24, and RT112 bladder cancer cells. β -actin was used as a loading control. **B)** ^{18}F -labeled galactodendritic unit 4 binding to UMUC3, UMUC14, HT1197, T24, and RT112 bladder cancer cells. $*P < 0.05$, $**P < 0.001$ determined by ANOVA comparing different bladder cancer cells. ANOVA was followed by Tukey *post hoc* multiple comparison analysis to determine statistical significance. **C)** ^{18}F -labeled galactodendritic unit 4 binding to UMUC3 bladder cancer cells before and after galectin-1 knockdown. Data are shown as mean %radioactivity / mg protein \pm S.E.M from three independent experiments ($**P < 0.01$ based on a Student's *t*-test and compared with UMUC3 cells). Scr, scrambled siRNA.

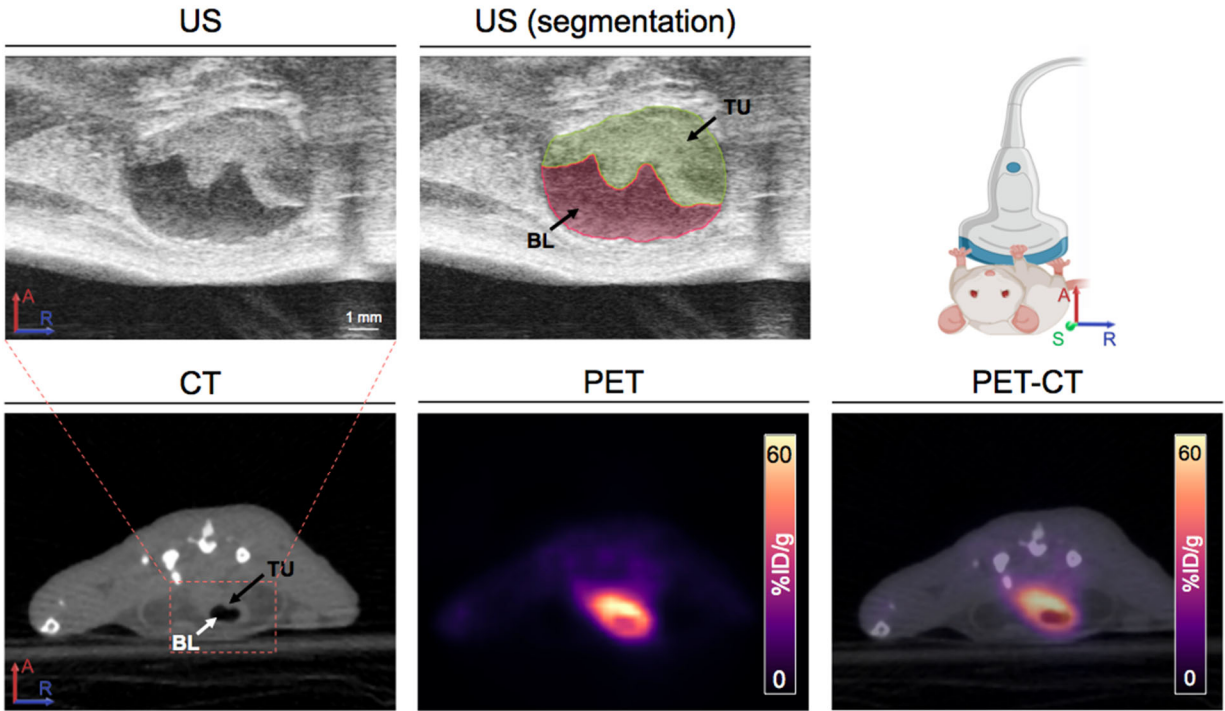
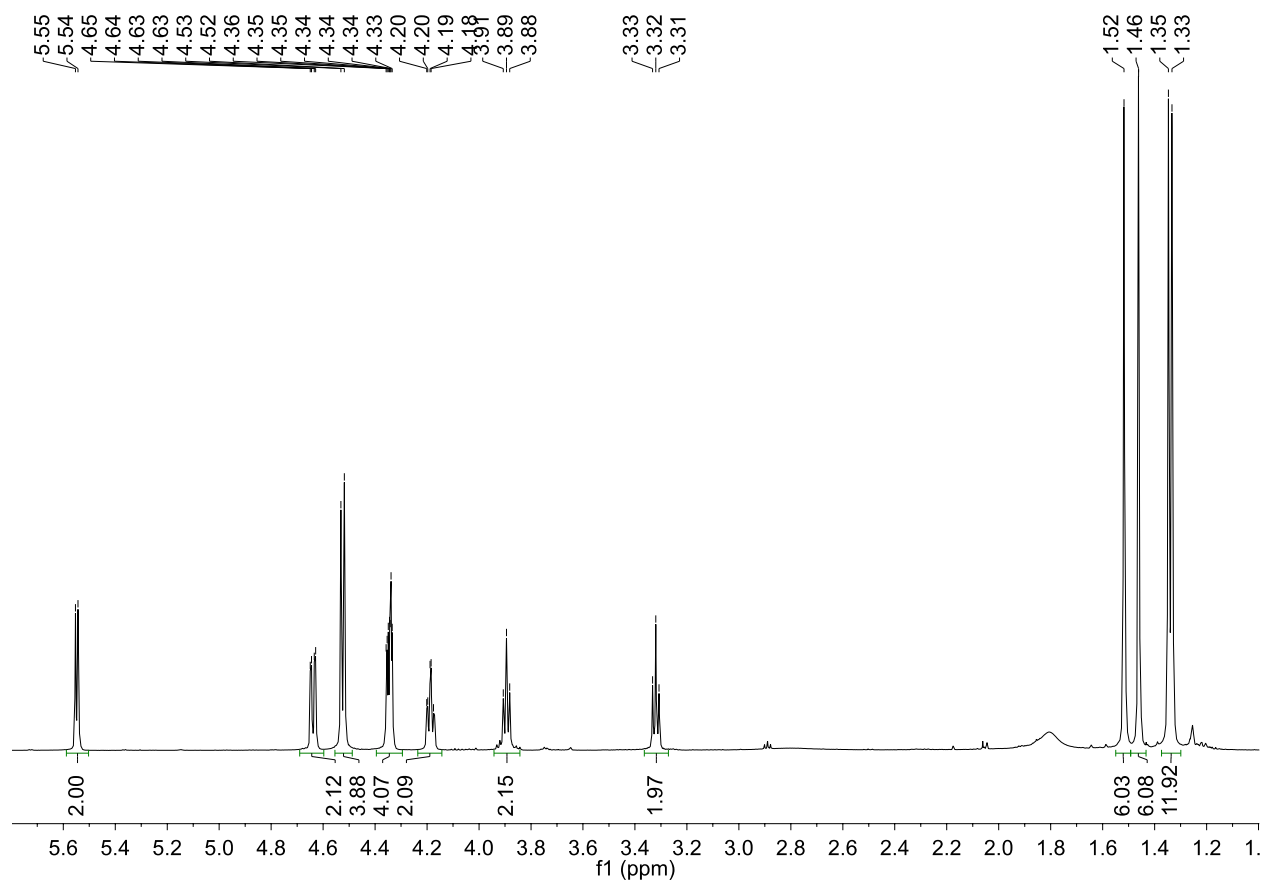
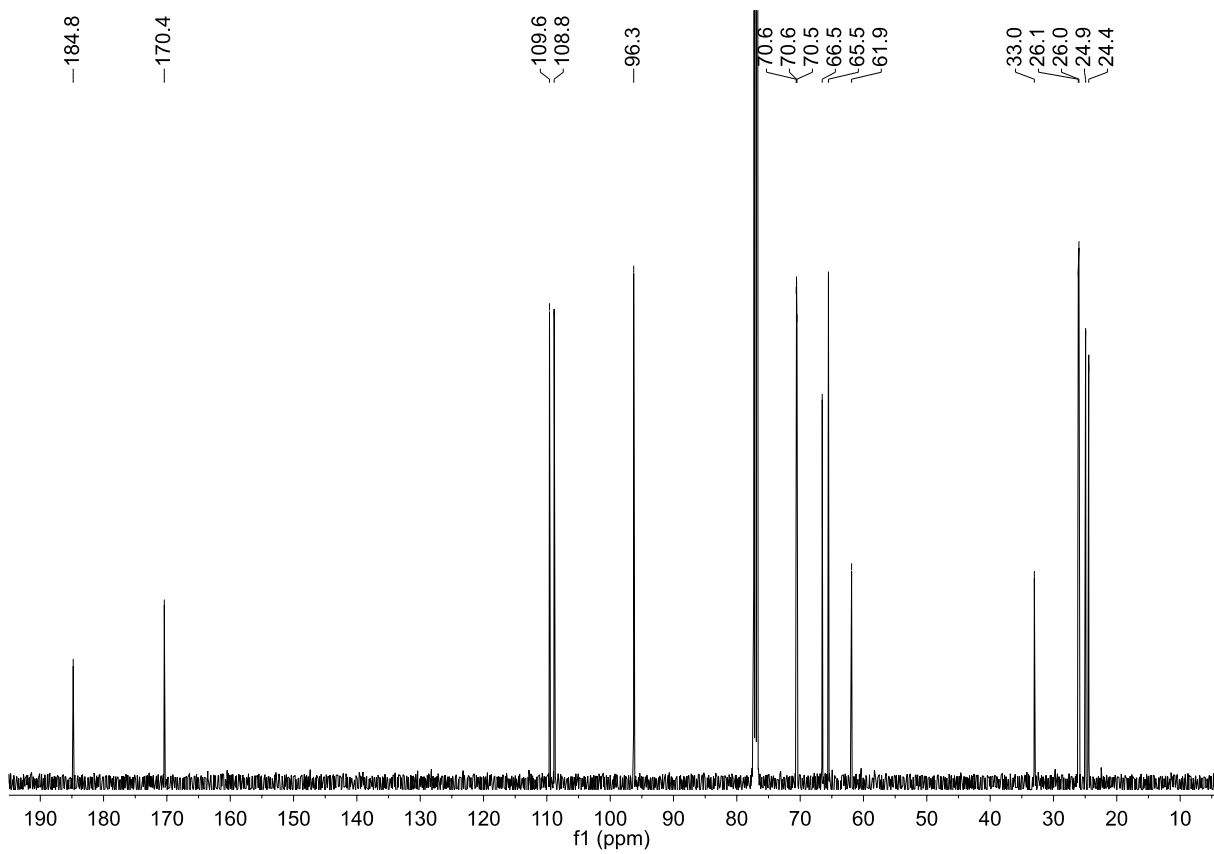


Figure 4. Top panel, Ultrasound images of murine bladders at 15 days after UMUC3 cells' implantation in the bladder. Lower panel, Representative axial PET/CT images at 1 h after administration of ^{18}F -labeled galactodendritic unit 4 in orthotopic UMUC3 bladder tumors. US, ultrasound; BL, bladder; TU, tumor; CT, Computer Tomography; PET, Positron Emission Tomography.

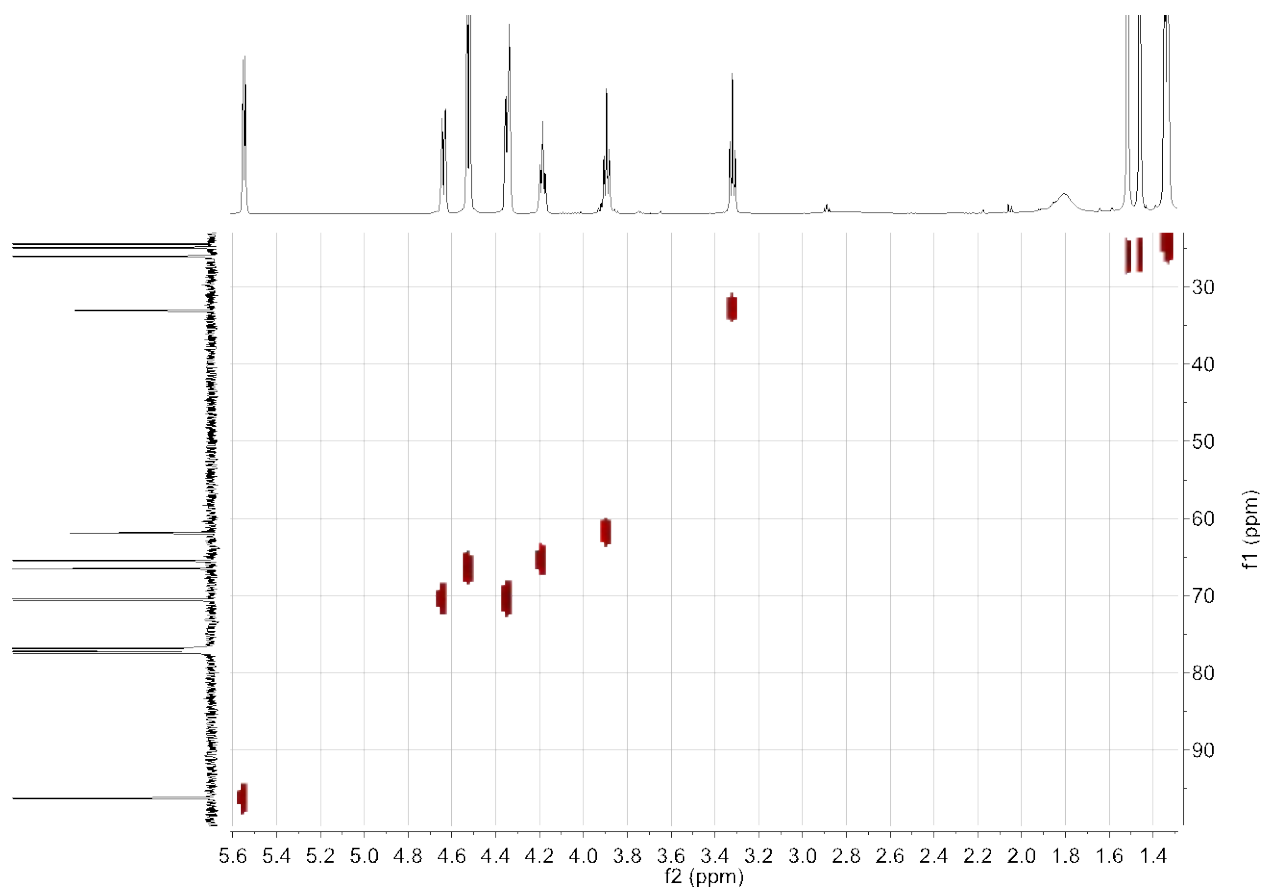
Supplementary Data for Pereira et al: PET/CT imaging with a ^{18}F -labeled galactodendritic carbohydrate in a galectin-1 overexpressing orthotopic bladder cancer model



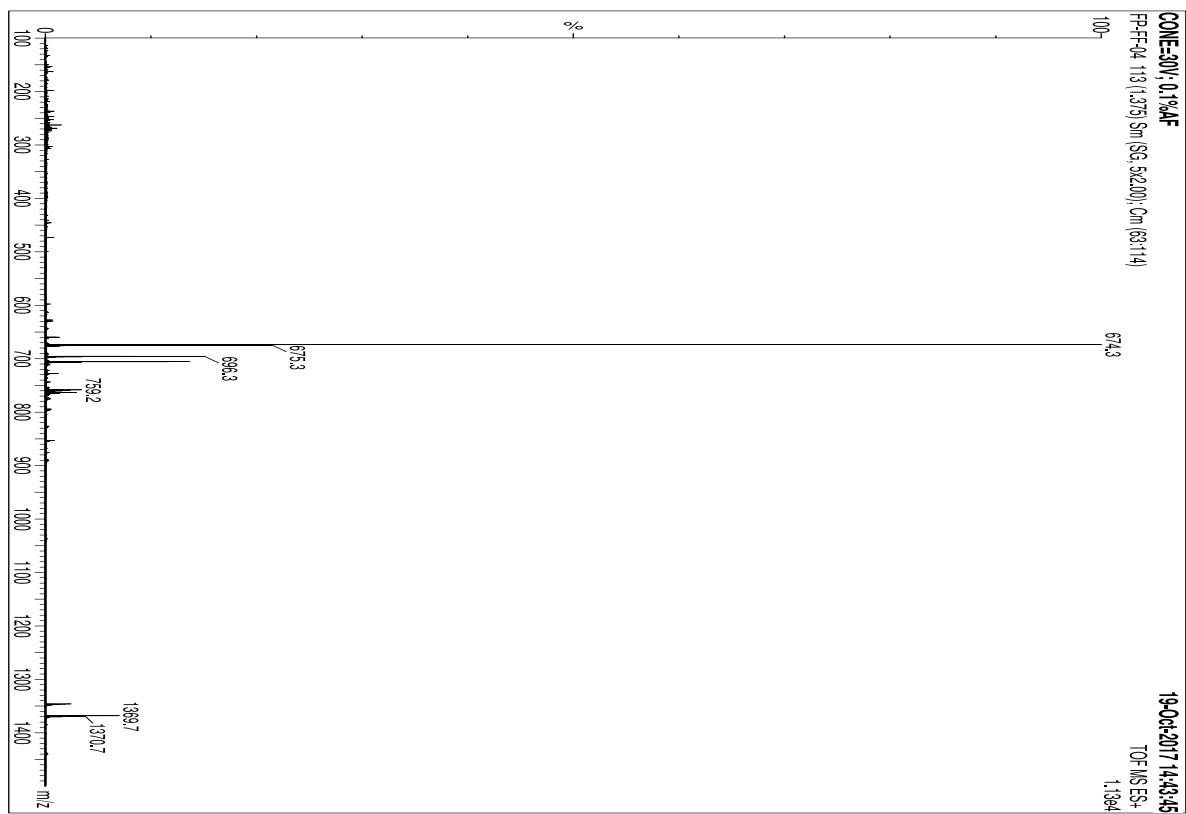
Supplementary Figure 1. ^1H NMR spectra of compound **1**. Compound **1** was dissolved in chloroform-*d* and ^1H NMR spectra acquired at 500 MHz. The full interpretation of the data is in the results section of the manuscript.



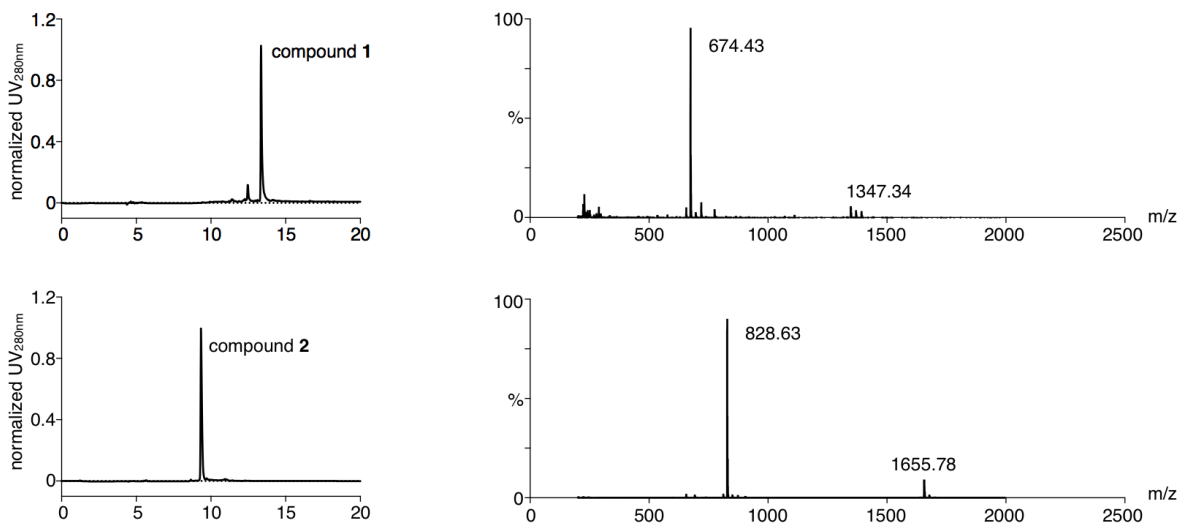
Supplementary Figure 2. ^{13}C NMR spectra of compound **1**. Compound **1** was dissolved in chloroform-*d* and ^1H NMR spectra acquired at 500 MHz. The full interpretation of the data is in the results section of the manuscript.



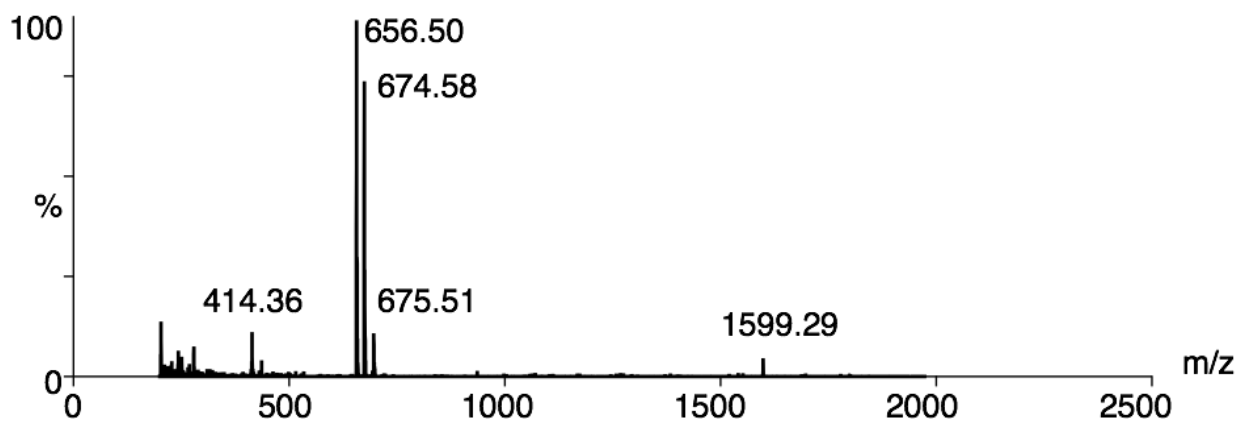
Supplementary Figure 3. Heteronuclear Single Quantum Coherence (HSQC) spectra of compound **1** to determine proton-carbon single bond correlations. Protons lie along the observed x-axis and carbons lie along the observed y-axis. Full interpretations of the data allowed for the full C-H structure determination of the compound reported in the results section of the manuscript.



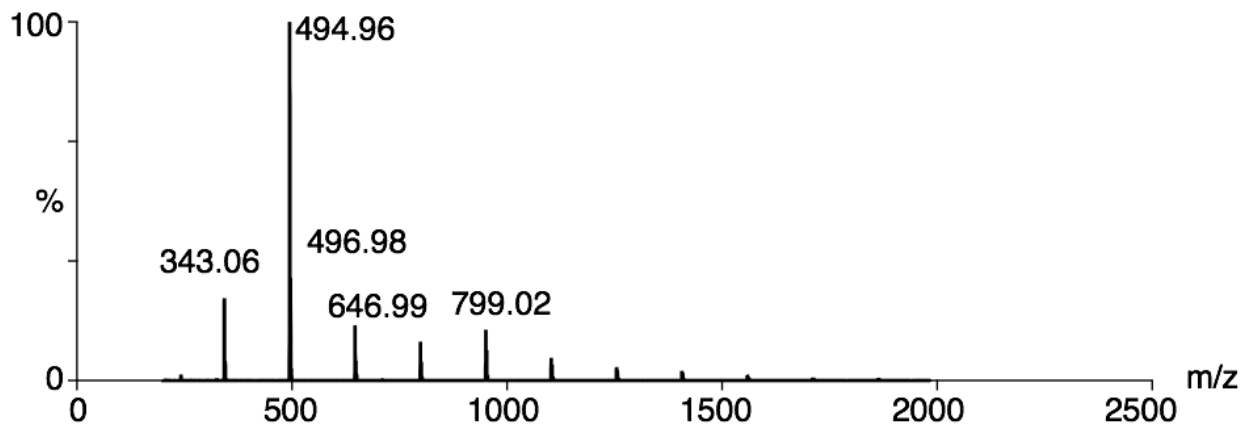
Supplementary Figure 4. Electrospray ionization mass spectrometry (ESI-MS) spectra of compound **1**. Calculated mass to charge ratio (m/z) for compound **1** was 673.25 and mass found was 674.3 $[M + H]^+$.



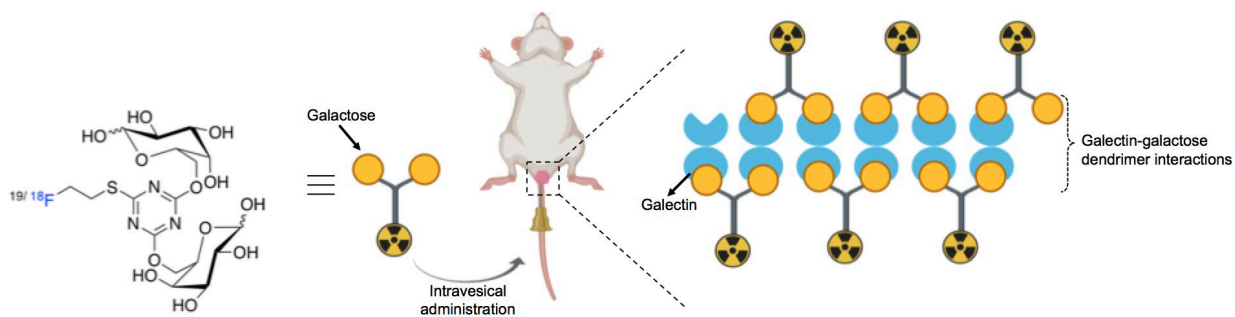
Supplementary Figure 5. HPLC chromatogram (*left*) ESI-MS spectra (*right*) of compound **1** and compound **2**. Calculated mass to charge ratio (m/z) for compound **2** was 827.26 and mass found 828.63 $[M + H]^+$.



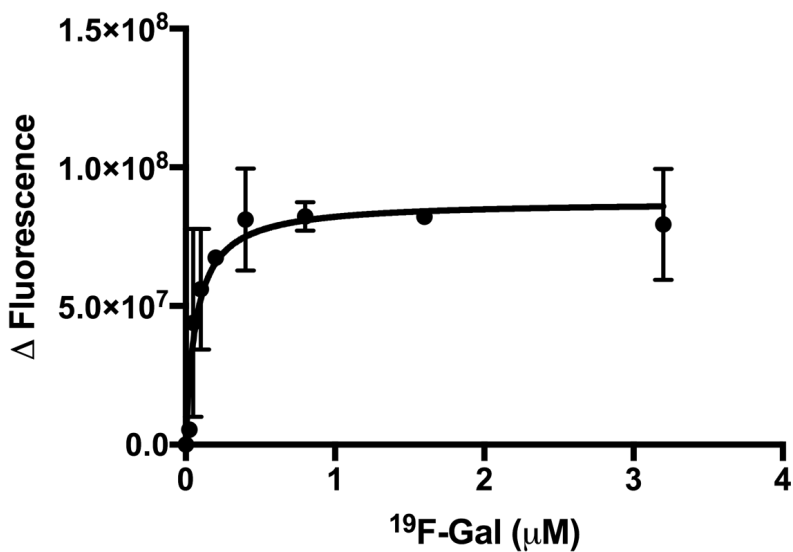
Supplementary Figure 6. ESI-MS spectra of compound **3**. Calculated mass to charge ratio (m/z) for compound **3** was 656.25 and mass found 656.50 $[M + H]^+$.



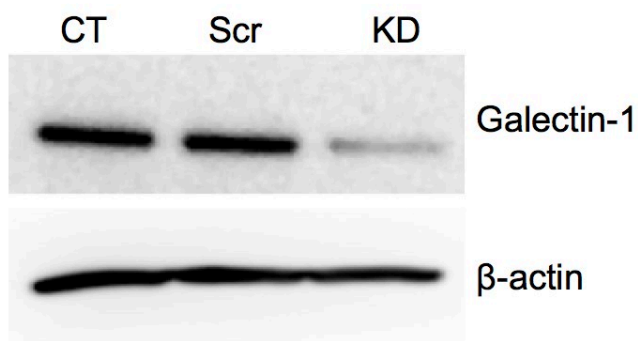
Supplementary Figure 7. ESI-MS spectra of compound **4**. Calculated mass to charge ratio (m/z) for compound **3** was 496.12 and mass found 496.98 $[M + H]^+$.



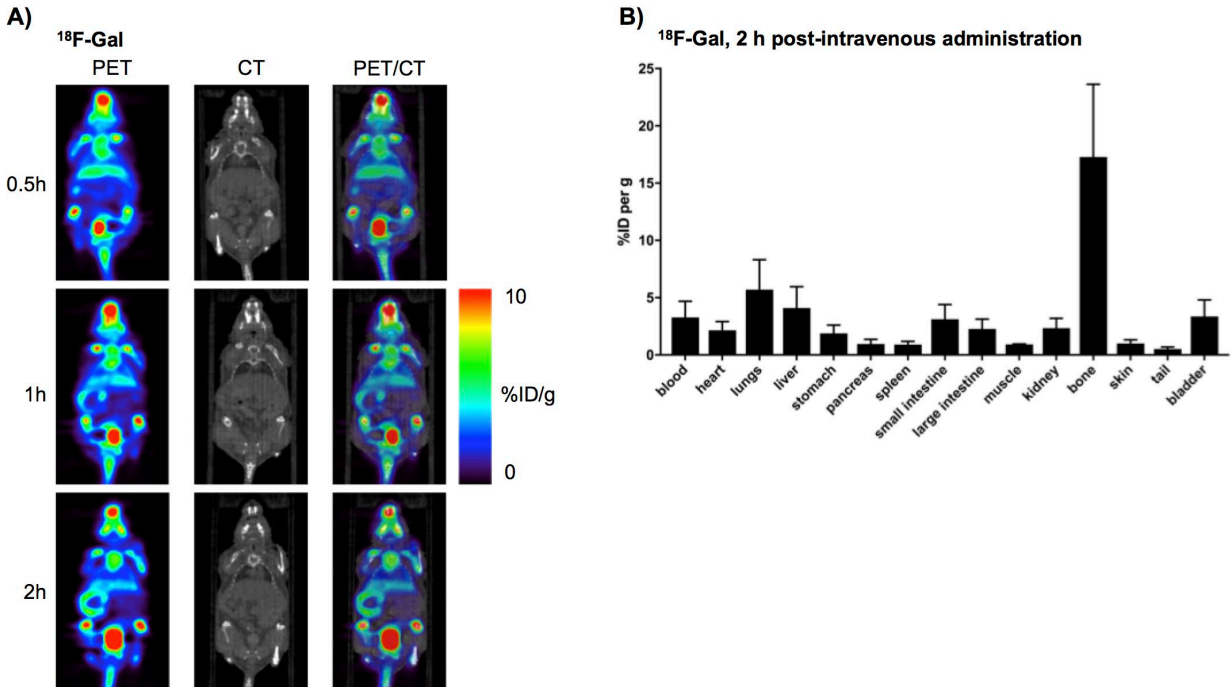
Supplementary Figure 8. The F-18 containing galactodendritic unit **4** was administered via intravesical injections into the bladder of mice bearing orthotopic UMUC3 bladder cancer cells. The galactose dendritic moieties in ^{18}F -labeled galactodendritic unit **4** interact with galectin-1 at the tumor cells, allowing BCa PET imaging.



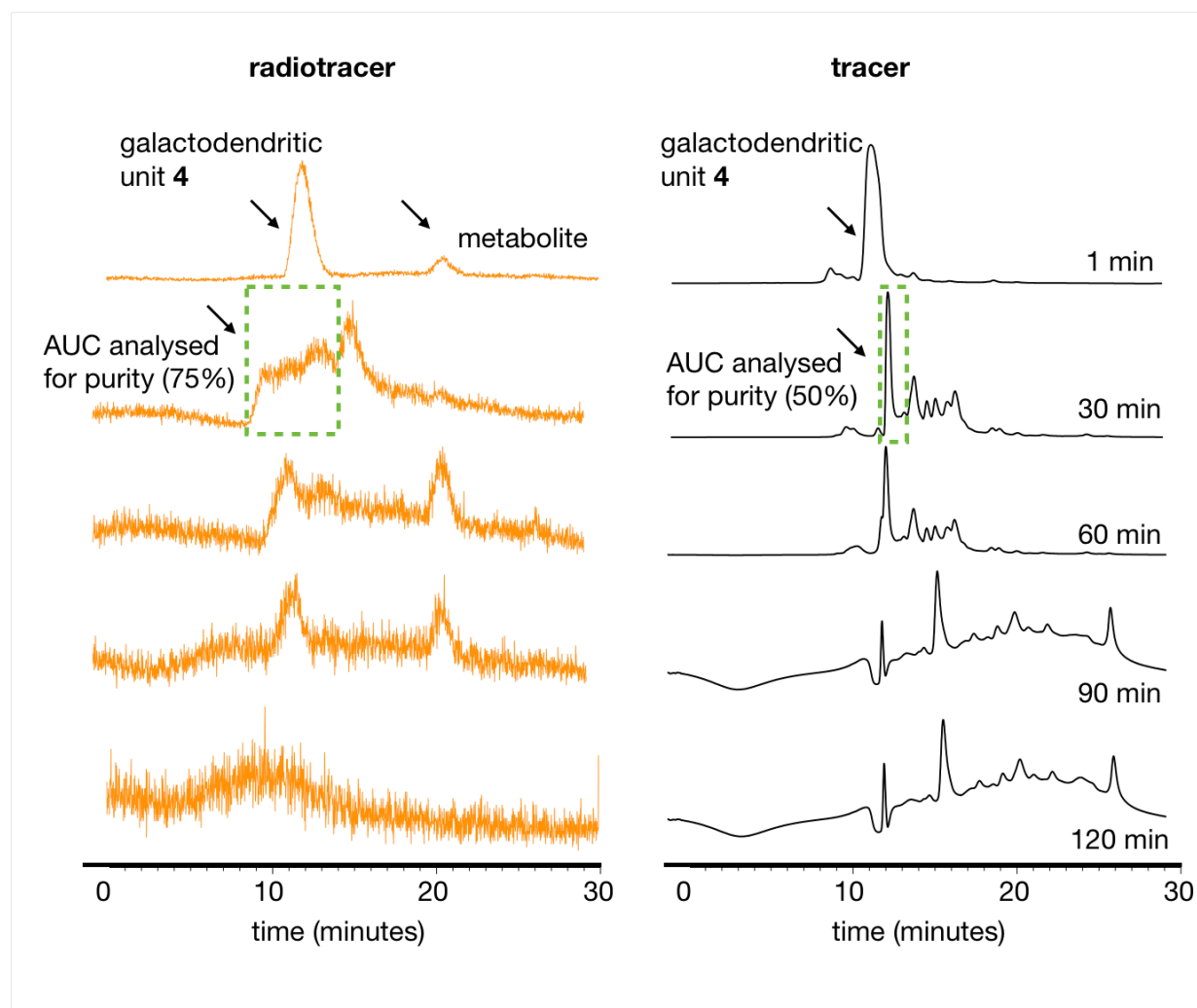
Supplementary Figure 9. Fluorescence variation on the emission spectrum of 2 μM galectin-1 protein after the addition of [^{19}F]compound 4. Data are means \pm S.E.M. of three independent experiments.



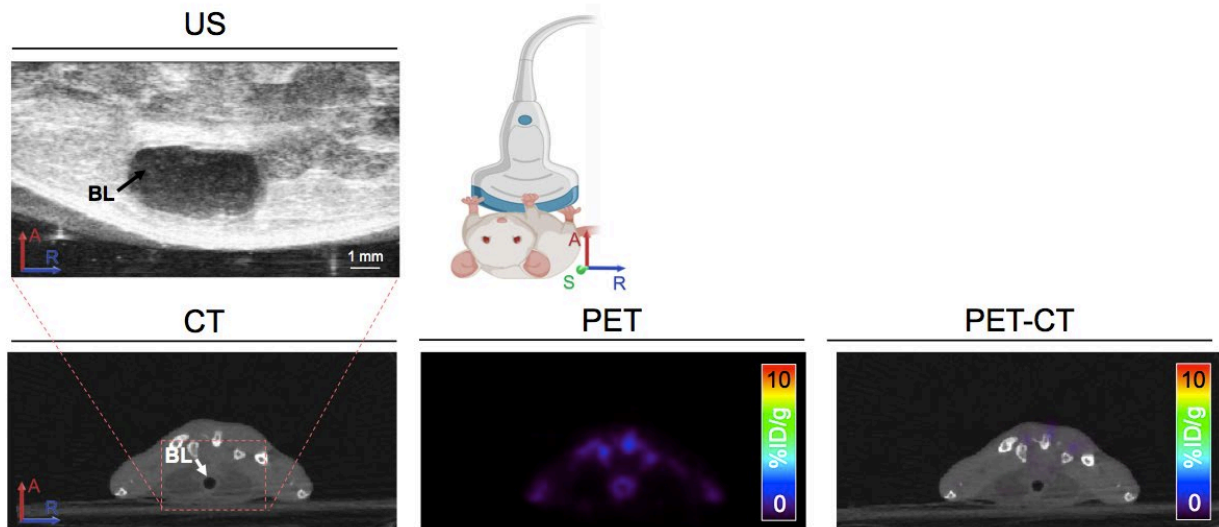
Supplementary Figure 10. Western blot analysis of galectin-1 in the total lysates of UMUC3 before and after knockdown using siRNA. Scr, scrambled siRNA.



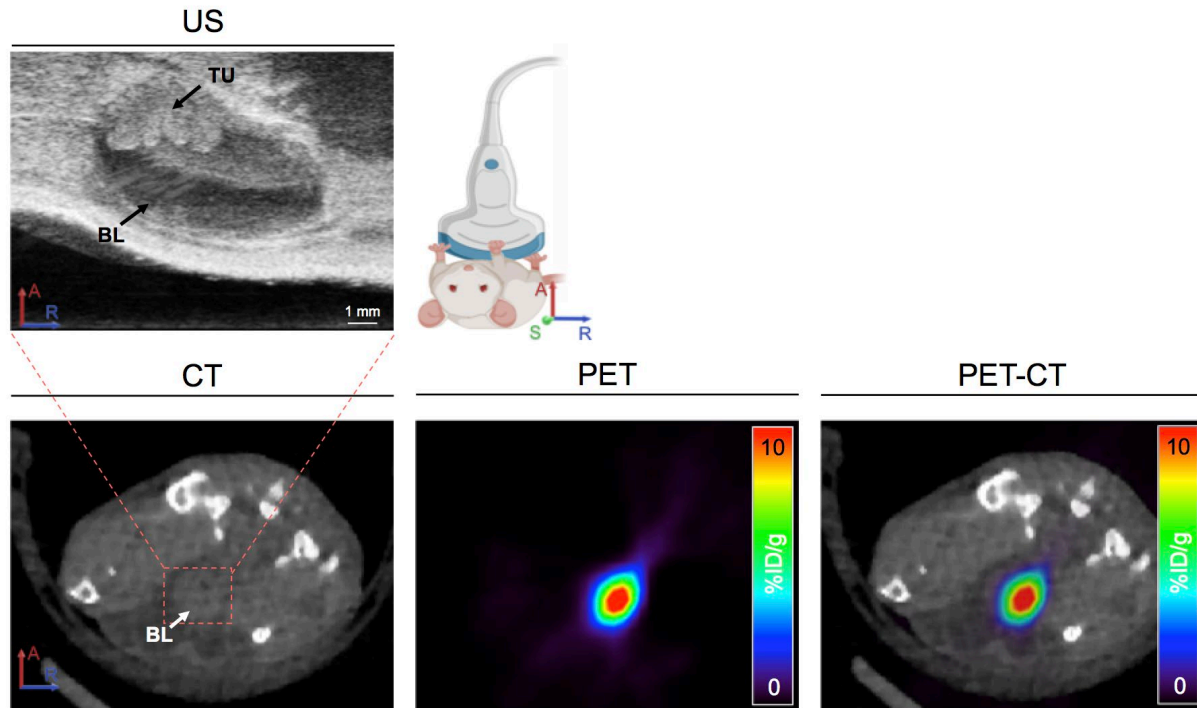
Supplementary Figure 11. (A) Representative coronal PET images and (B) biodistribution data of ¹⁸F-labeled galactodendritic unit 4 in athymic nude mice bearing orthotopic UMUC3 bladder tumors. Mice were intravenous administrated ¹⁸F-labeled galactodendritic unit 4 (2.9 – 3.3 MBq) and PET/CT images acquired at 0.5, 1, and 2 h post-administration of the galactose radiotracer. Biodistribution was performed at 2 h post-injection of ¹⁸F-labeled galactodendritic unit 4 (Bars, $n = 4$ mice per group, mean \pm S.E.M). CT, Computer Tomography; PET, Positron Emission Tomography; %ID/g, percentage of injected dose per gram of tissue.



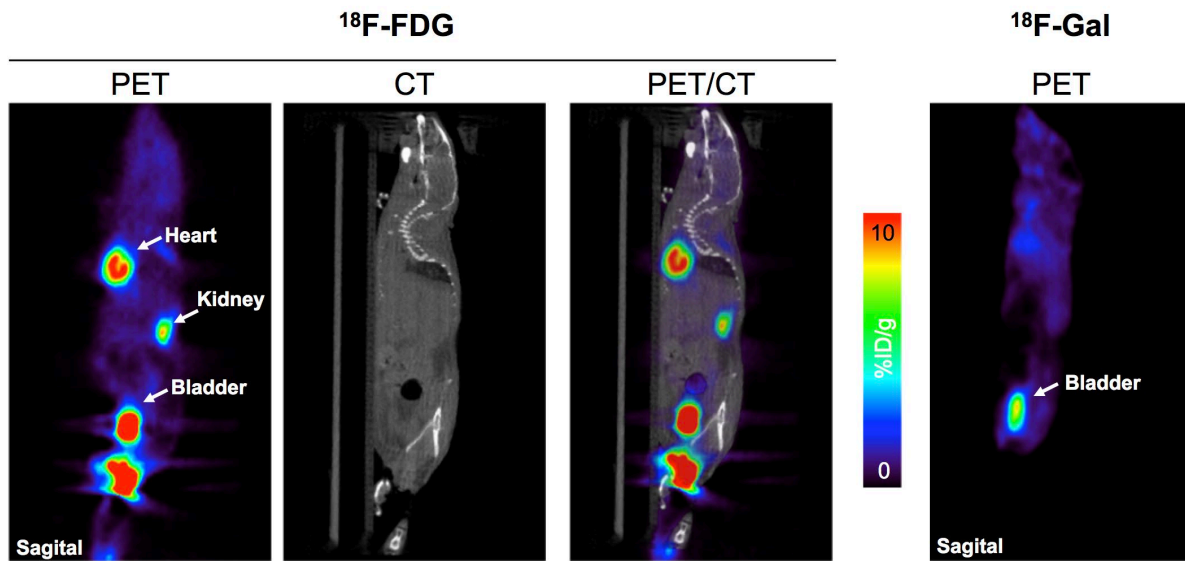
Supplementary Figure 12. Stability of ^{18}F -labeled galactodendritic unit **4** in saline sample containing 10.5% (v/v) mice urine. **(left)** Radiotracer chromatogram of ^{18}F -labeled galactodendritic unit **4** in a saline sample containing mice urine at various time-points post-incubation (1 min, 30 min, 60 min, 90 min, and 120 min). **(right)** Corresponding HPLC chromatogram (280 nm) of ^{18}F -labeled galactodendritic unit **4** in a saline sample containing mice urine at various time-points post-incubation (1 min, 30 min, 60 min, 90 min, and 120 min). AUC, area under the curve.



Supplementary Figure 13. Top panel, Ultrasound image of murine bladders of non-tumor bearing mice. Lower panel, Representative axial PET images at 1 h after administration of ^{18}F -labeled galactodendritic unit 4 in athymic nude mice. Mice were intravesical administrated ^{18}F -labeled galactodendritic unit 4 (14.7 – 15.3 MBq), the bladder was flushed with PBS, and PET/CT images were acquired at 1 h post-administration of the galactose radiotracer. US, ultrasound; BL, bladder; TU, tumor; CT, Computer Tomography; PET, Positron Emission Tomography.



Supplementary Figure 14. Top panel, Ultrasound images of murine bladders at 15 days after UMUC3 cells' implantation in the bladder. **Lower panel**, Representative axial PET images at 1 h after administration of ^{18}F -FDG in athymic nude mice bearing orthotopic UMUC3 bladder tumors. Mice were intravesical administrated ^{18}F -FDG (14.7 – 15.3 MBq), the bladder flushed with PBS, and PET/CT images acquired at 1 h post-administration of the glucose radiotracer. US, ultrasound; BL, bladder; TU, tumor; CT, Computer Tomography; PET, Positron Emission Tomography.



Supplementary Figure 15. Representative sagittal PET images of (left) ^{18}F -FDG and (right) ^{18}F -labeled galactodendritic unit 4 in athymic nude mice bearing orthotopic UMUC3 bladder tumors. Mice were intravesical administrated ^{18}F -FDG or ^{18}F -labeled galactodendritic unit 4 (14.7 – 15.3 MBq), the bladder was flushed with PBS, and PET/CT images were acquired at 1 h post-administration of the glucose or galactose radiotracer. CT, Computer Tomography; PET, Positron Emission Tomography.